The Dynamic Beamformer

Ali Bahramisharif[1,2,⋆], Marcel A.J. van Gerven[2,1], Jan-Mathijs Schoffelen[2], Zoubin Ghahramani[3], and Tom Heskes[1,2]

[1] Radboud University Nijmegen, Institute for Computing and Information Sciences, Nijmegen, The Netherlands
ali@cs.ru.nl
[2] Radboud University Nijmegen, Donders Institute for Brain, Cognition and Behaviour, Nijmegen, The Netherlands
[3] Department of Engineering, University of Cambridge, Cambridge, UK

Abstract. Beamforming is one of the most commonly used methods for estimating the active neural sources from the MEG or EEG sensor readings. The basic assumption in beamforming is that the sources are uncorrelated, which allows for estimating each source independent of the others. In this paper, we incorporate the independence assumption of the standard beamformer in a linear dynamical system, thereby introducing the dynamic beamformer. Using empirical data, we show that the dynamic beamformer outperforms the standard beamformer in predicting the condition of interest which strongly suggests that it also outperforms the standard method in localizing the active neural generators.

1 Introduction

As the number of possible neural sources is much higher than the number of MEG or EEG sensor readings, the inverse problem of estimating source amplitudes from sensor readings has many solutions. A common approach to tackle this problem is to assume that all sources are independent from each other. This approach is widely used in the neuroscience community and is known as beamforming [6–9].

Since the source amplitude is likely to change smoothly over time, we expect to improve the source localization by taking the temporal dynamics into account. Smoothness constraints have been combined with source localization in a Bayesian framework [12, 16, 19]. Furthermore, source localization with a multivariate autoregressive source model has been presented in [10], where the sources are assumed to be independent and identically distributed in time and the components are subject to non-Gaussian distributions. The Kalman filter and particle filter have also been introduced in the context of EEG and MEG source localization based on dipole-fitting approaches [1, 2]. The model introduced in [1, 2] relies on the integration of many dynamic dipolar neural models. In this paper, in contrast to the previous methods, we start from the standard

⋆ Corresponding author. The authors gratefully acknowledge the support of the BrainGain Smart Mix Programme of the Netherlands Ministry of Economic Affairs and the Netherlands Ministry of Education, Culture and Science.

G. Langs et al. (Eds.): MLINI 2011, LNAI 7263, pp. 148–155, 2012.

beamforming solution and we show that we can incorporate the independence assumption of the standard beamformer in a linear dynamical system. We demonstrate that by using the leadfield matrix as the observation model and setting the covariance of the observation noise proportional to the covariance of the observation, we arrive at the dynamic beamformer.

2 Method

2.1 Beamforming

Let m, n, and T denote the number of sources, sensors, and samples, respectively. The goal of source localization is to estimate active sources $S \in \mathbb{R}^{m \times T}$ from sensor readings $X \in \mathbb{R}^{n \times T}$. In the source localization problem, sources are assumed to project linearly to the sensors via a leadfield matrix $L \in \mathbb{R}^{n \times m}$. In other words, $X = LS$, where L and X are given and S is to be estimated. If we further assume that the solution to the source localization problem can be written as a linear mapping from sensors to sources, the problem of source localization reduces to estimating the linear projection matrix $W \in \mathbb{R}^{n \times m}$ that projects the sensors to the sources; in other words: $S = W'X$.

Beamforming derives from the assumption that the sources are uncorrelated. Defining $\mathbf{s}_i \equiv S_{i\cdot}, \boldsymbol{\ell}_i \equiv L_{\cdot i}$, and $\mathbf{w}_i \equiv W_{\cdot i}$, for each source $\mathbf{s}_i \equiv (\mathrm{s}_{i,1}, \ldots, \mathrm{s}_{i,T})$, we can write: $\mathbf{s}_i = \mathbf{w}_i' X = \mathbf{w}_i' \boldsymbol{\ell}_i \mathbf{s}_i$, which implies that $\mathbf{w}_i' \boldsymbol{\ell}_i = 1$ for all $i \in 1, \ldots, m$. A standard approach is to minimize the variance of the sources and find the $\mathbf{w}_i$ which minimizes $\mathbf{s}_i \mathbf{s}_i' = \mathbf{w}_i' \Sigma \mathbf{w}_i$ subject to $\mathbf{w}_i' \boldsymbol{\ell}_i = 1$, where $\Sigma \equiv XX'$. The solution is shown to be [18]:

$$\mathbf{s}_i = (\boldsymbol{\ell}_i' \Sigma^{-1} \boldsymbol{\ell}_i)^{-1} \boldsymbol{\ell}_i' \Sigma^{-1} X \tag{1}$$

for all $i \in 1, \ldots, m$.

2.2 Linear Gaussian Model

The beamformer can be interpreted as a specific kind of linear probabilistic model. Assume that we have a linear Gaussian model, as shown in Fig. 1a, in which $\mathbf{x}_t \equiv X_{\cdot t}$ is the observation at time t where $1 \leq t \leq T$, and $\boldsymbol{\ell}_i$ is given. Sensor observations linearly depend on source activations through $\mathbf{x}_t = \boldsymbol{\ell}_i \mathrm{s}_{i,t} + \mathbf{u}_{i,t}$, where $\mathbf{u}_{i,t} \sim \mathcal{N}(0, R)$. Now we try to find $\mathbf{s}_i$ which maximizes the likelihood of the parameters given the observations and R. Ignoring the constant terms, the negative log-likelihood can be written as $\frac{1}{2}(X - \boldsymbol{\ell}_i \mathbf{s}_i)' R^{-1} (X - \boldsymbol{\ell}_i \mathbf{s}_i)$, which is minimized by

$$\mathbf{s}_i = \left(\boldsymbol{\ell}_i' R^{-1} \boldsymbol{\ell}_i\right)^{-1} \boldsymbol{\ell}_i' R^{-1} X \,. \tag{2}$$

Comparing Eqs. 1 and 2, we see that with R proportional to Σ, the model depicted in Fig. 1a is equivalent to the standard beamformer. In other words, a linear Gaussian model is a beamformer if we assume that the covariance of the observation noise is proportional to the covariance of the observations and use the leadfield matrix as the observation model.

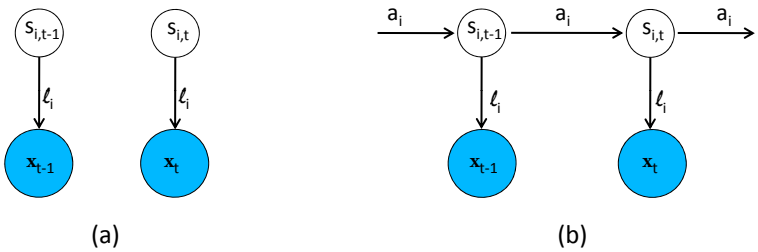

Fig. 1. (a) Graphical representation of a linear Gaussian model. (b) Graphical representation of the dynamic beamformer.

2.3 Dynamic Beamforming

The correspondence between the beamformer and the linear Gaussian model suggests that a similar correspondence can be exploited using a linear dynamical system. We introduce the dynamic beamformer, which can be obtained by just using the leadfield matrix as the observation model of a linear dynamical system and setting the covariance of the observation noise to be proportional to the covariance of the observation. The graphical model of the dynamic beamformer is shown in Fig. 1b. For each source $\mathbf{s}_i \equiv (\mathrm{s}_{i,1}, \ldots, \mathrm{s}_{i,T})$, dynamic beamforming can be mathematically expressed as

$$\mathbf{x}_t = \boldsymbol{\ell}_i \mathrm{s}_{i,t} + \mathbf{u}_{i,t} \tag{3}$$

$$\mathrm{s}_{i,t} = \mathrm{a}_i \mathrm{s}_{i,t-1} + v_{i,t} \tag{4}$$

where $\mathbf{u}_{i,t} \sim \mathcal{N}(0, \alpha_i \Sigma)$ and $v_{i,t} \sim \mathcal{N}(0, q_i)$ independently for $i \in 1, \ldots, m$ and $1 \leq t \leq T$. Note that $\mathrm{s}_{i,t}$, a_i, q_i, and α_i are scalar values. Note further that each $\mathbf{s}_i$ should be predictive for the full observation X, so there is no i in the left side of Eq. 3. Following the equations reported in [17], we can find a_i, q_i, α_i, and $\mathbf{s}_i$ by means of an expectation maximization algorithm. We use both filtering and smoothing (forward and backward) equations to have a better estimate of the sources.

2.4 Empirical Data

We evaluated our method using MEG data of the best performing subject reported in [3]. The subject's task was to maintain central fixation while covertly attending to a target which followed a circular trajectory. The condition was given by the sine and cosine of the angles between the target and the positive x-axis over time. To construct the leadfield matrix, we used a structural MRI and the head model developed in [13]. Then we discretized the brain volume into a grid with $1 \times 1 \times 1\,\mathrm{cm}^3$ resolution. For each grid point the leadfield was calculated. Preprocessing and leadfield generation was done using FieldTrip [14].

The complexity of the dynamic beamformer increases with the number of time points. As shown in [3], task-specific information for this data shows up

as modulations of occipital alpha power (8-12 Hz) in the frequency domain. Applying the dynamic beamformer on the frequency domain results in a much lower processing time. In this study we used a linear trick for power extraction in order not to violate the linearity of the beamformer. Imagine that we have a reference signal which has the same frequency and the same phase as the signal that we want to decode. We take the Fourier transform of the data, which is a linear operation, only focusing on the desired frequency, and subtract the phase of the reference signal. Then, the real part of the Fourier transform would represent the amplitude of the signal which, averaged over a time window, results in an estimate of the power of the signal over that frequency [15]. As the reference signal we chose the average signal over eight channels which showed the highest average alpha power. For the Fourier transform, we used a 500 ms time window. To include all variations of the alpha band in predicting the conditions, there was a 400 ms overlap between the consecutive trials.

2.5 Validation

Brain source localization is difficult to validate as mostly there is no certain knowledge about the exact location of the active sources. In this paper, we validated our method by decoding the experimental design from the source estimates. We used 25 minutes of data for training and 5 minutes for testing our algorithm. To optimize parameters based on the training set, we used a two-fold cross-validation approach, i.e., the first half (12.5 minutes) for training and the second half for testing and vice versa. After optimizing parameters, we computed the performance on the test set. We used the correlation between the actual and predicted sine and cosine of the angle as the performance measure.

We validated our beamformer results using two different approaches: a stationary and a dynamic approach. The stationary validation approach uses two

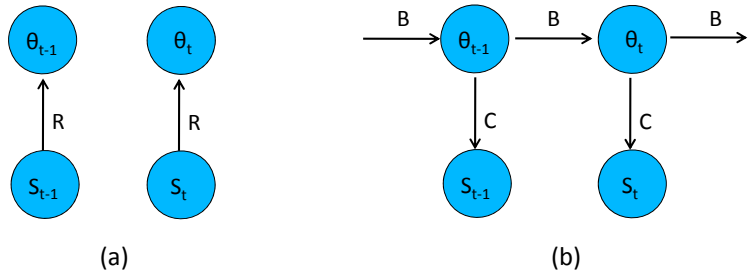

Fig. 2. (a) Graphical representation of the linear regression model used to predict the direction of attention from the reconstructed sources. R stand for the regression coefficients. (b) Graphical representation of the linear dynamical system used to predict the direction of attention from the reconstructed sources. B and C stand for the state transition matrix and the observation model in the linear dynamical system, respectively.

L2 regularized linear regressors to predict sine and cosine of the direction of attention from the alpha sources. Showing sine and cosine of the direction of attention with $\Theta \in \mathbb{R}^{2\times T}$, we obtain the graphical representation of our linear regression model as shown in Fig. 2a.

From the experimental design reported in [3], we know that the direction of attention changes smoothly over time. That is, the predicted direction of attention not only depends on the alpha activity but is also highly related to the previous predicted direction. In our dynamic validation approach, we model this smoothness assumption again in a linear dynamical system framework. The graphical representation of this model is presented in Fig. 2b. Using data of the training set and again following the equations reported in [17], we can learn the parameters of this model and use it for predicting the conditions of the test set.

3 Results and Discussion

We computed the absolute correlation of the sources reconstructed using both the beamformer and the dynamic beamformer with the experimental design which, in our case, is given by the sine and cosine of the direction of attention. As shown in Fig. 3a, occipital sources are more correlated with the experimental design in the dynamic beamformer reconstruction. These occipital sources are known to be involved when subjects are covertly attending to a peripheral target [4]. Here, the higher correlation is expected, as the experimental design changes very smoothly and the dynamic beamformer enforces the smooth transition of the sources which results in a higher correlation.

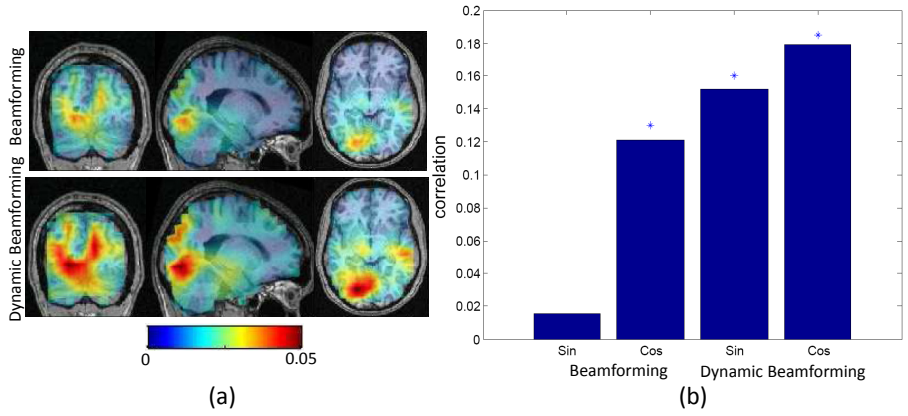

Fig. 3. (a) Correlation of the sources reconstructed using both the beamformer and the dynamic beamformer with the experimental conditions. (b) Correlation between actual and predicted experimental design based on the sources reconstructed using either the beamformer or the dynamic beamformer. Significant correlations ($p < 0.001$) are marked with a '*'.

Following the stationary validation approach, we show the prediction results using two L2 regularized linear regressors. Figure 3b shows the correlation of the predictions for sine and cosine based on the sources reconstructed using the beamformer and the dynamic beamformer with the true values. As shown, the dynamic beamformer results in a better prediction of the conditions than the standard beamformer. Specifically, the dynamic beamformer is performing much better for the sine component of the angle than the standard version. As the sign of the cosine and sine represent left versus right and up versus down, respectively, Fig. 3b implies that it is more difficult to discriminate up from down than left from right using the sources reconstructed with standard beamforming. Furthermore, if we look at the absolute regression coefficients obtained by either standard or dynamic beamforming shown in Fig. 4, we see that only the regression coefficients of the dynamic beamformer are consistent with the correlations shown in Fig. 3a. As the trained regressor on the sources reconstructed from standard beamforming focuses on the task-irrelevant brain regions, the poor performances of the beamforming part of Fig. 3b is expected.

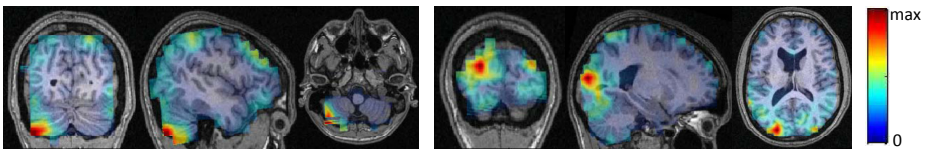

Fig. 4. Average absolute value of the regression coefficients for predicting sine and cosine of the direction of attention using the sources obtained by (a) standard beamforming and (b) dynamic beamforming

We further checked whether we could improve predictive performance by making use of a linear dynamical system on the dynamic beamformer results following the dynamic validation approach. Having the sources reconstructed from the dynamic beamformer, based on the training data, we sorted the sources according to their correlation with the experimental condition. We then checked whether we need all the sources to have a good prediction. Using a linear dynamical system on a subset of sources, from 1 to 500 sources, we show how the average absolute correlation between the predictions and the true directions changes in Fig. 5a. As the performance drops dramatically by adding more sources than 400, we did not go beyond analyzing 500 sources. It can be seen in Fig. 5a that the optimal number of sources to be used for predicting the direction of attention is about 300. Using a linear dynamical system on the 300 sources, the prediction result is shown in Fig. 5b. This result is equivalent to a correlation of 0.42 for sine and 0.58 for cosine compared to the results shown in Fig. 3b. In other words, making use of a linear dynamical system on a subset of sources, the prediction of the experimental condition becomes about three times better than using two linear regressors. The predictions are consistent with the results shown in [11].

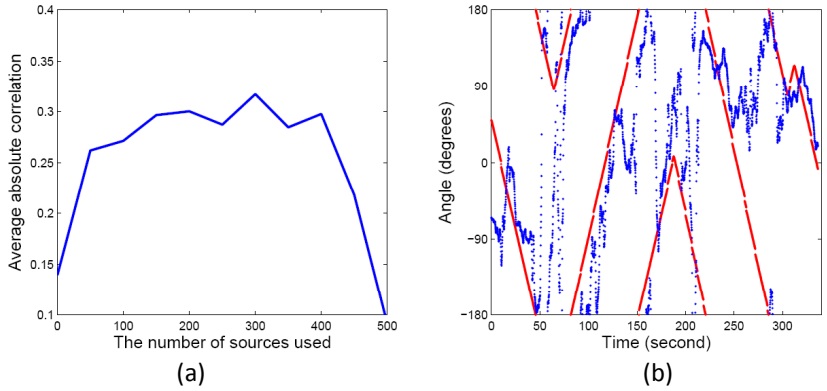

Fig. 5. (a) Average absolute correlation between the experimental condition and the predictions using a linear dynamical system model. (b) The prediction on the test set using 300 sources. Red dots show the true angle and blue dots show the predictions.

4 Conclusion

In this paper, we showed that we can incorporate the independence assumption of the standard beamformer in a linear dynamical system by using the leadfield matrix as the observation model and setting the covariance of the observation noise to be proportional to the covariance of the observation. This led to our formulation of the dynamic beamformer. We evaluated our method using an MEG dataset reported in [3]. We validated our method by decoding the experimental design from the sources extracted using both the standard beamformer and the dynamic beamformer. Our validation as shown in Fig. 3b, demonstrated that the dynamic beamformer outperforms the standard beamformer in predicting the direction to which a subject was covertly attending. We further showed in Fig. 5 that we can improve the prediction of the attended direction from the sources by making use of a linear dynamical system. Our results strongly suggest that the dynamic beamformer outperforms the standard approach in estimating the active neural generators. Further Bayesian optimization approaches other than the maximum likelihood can be applied to improve the performance of the dynamic beamformer in future studies [5].

References

1. Antelis, J., Minguez, J.: Dynamic solution to the EEG source localization problem using Kalman filters and particle filters. In: Annual International Conference of the IEEE Engineering in Medicine and Biology Society (EMBC), pp. 77–80 (2009)
2. Antelis, J., Minguez, J.: DYNAMO: Dynamic multi-model source localization method for EEG and/or MEG. In: Annual International Conference of the IEEE Engineering in Medicine and Biology Society (EMBC), pp. 5141–5144 (2010)

3. Bahramisharif, A., van Gerven, M., Heskes, T., Jensen, O.: Covert attention allows for continuous control of brain-computer interfaces. Eur. J. Neurosci. 31(8), 1501–1508 (2010)
4. Beauchamp, M., Petit, L., Ellmore, T., Ingeholm, J., Haxby, J.: A parametric fMRI study of overt and covert shifts of visuospatial attention. NeuroImage 14(2), 310–321 (2001)
5. Bishop, C.: Pattern Recognition and Machine Learning. Springer (2006)
6. Dale, A., Liu, A., Fischl, B., Buckner, R., Belliveau, J., Lewine, J., Halgren, E.: Dynamic statistical parametric mapping: Combining fMRI and MEG for high-resolution imaging of cortical activity. Neuron 26(1), 55–67 (2000)
7. Dale, A., Sereno, M.: Improved localization of cortical activity by combining EEG and MEG with MRI cortical surface reconstruction: a linear approach. J. Cognitive Neurosci. 5(2), 162–176 (1993)
8. Gross, J., Kujala, J., Hämäläinen, M., Timmermann, L., Schnitzler, A., Salmelin, R.: Dynamic imaging of coherent sources: studying neural interactions in the human brain. P. Natl. Acad. Sci. USA 98(2), 694–699 (2001)
9. Hämäläinen, M., Ilmoniemi, R.: Interpreting magnetic fields of the brain: minimum norm estimates. Med. Biol. Eng. Comput. 32(1), 35–42 (1994)
10. Haufe, S., Tomioka, R., Nolte, G., Müller, K., Kawanabe, M.: Modeling sparse connectivity between underlying brain sources for EEG/MEG. IEEE T. Bio-Med. Eng. 57(8), 1954–1963 (2010)
11. Jensen, O., Bahramisharif, A., Oostenveld, R., Klanke, S., Hadjipapas, A., Okazaki, Y., van Gerven, M.: Using brain–computer interfaces and brain-state dependent stimulation as tools in cognitive neuroscience. Front. Psychol. 2(100) (2011)
12. Mattout, J., Phillips, C., Penny, W., Rugg, M., Friston, K.: MEG source localization under multiple constraints: an extended Bayesian framework. NeuroImage 30(3), 753–767 (2006)
13. Nolte, G.: The magnetic lead field theorem in the quasi-static approximation and its use for magnetoencephalography forward calculation in realistic volume conductors. Phys. Med. Biol. 48, 3637–3652 (2003)
14. Oostenveld, R., Fries, P., Maris, E., Schoffelen, J.: FieldTrip: open source software for advanced analysis of MEG, EEG, and invasive electrophysiological data. Computat. Intell. Neurosc. 2011, 1 (2011)
15. Oppenheim, A., Willsky, A., Nawab, S.: Signals and Systems. Pearson education (1998)
16. Penny, W., Kiebel, S., Friston, K.: Variational Bayesian inference for fMRI time series. NeuroImage 19(3), 727–741 (2003)
17. Roweis, S., Ghahramani, Z.: A unifying review of linear Gaussian models. Neural Comput. 11(2), 305–345 (1999)
18. Van Veen, B., van Drongelen, W., Yuchtman, M., Suzuki, A.: Localization of brain electrical activity via linearly constrained minimum variance spatial filtering. IEEE T. Bio-Med. Eng. 44(9), 867–880 (1997)
19. Wipf, D., Nagarajan, S.: A unified Bayesian framework for MEG/EEG source imaging. NeuroImage 44(3), 947–966 (2009)